

New physics couplings from angular coefficient functions of $\bar{B} \rightarrow D^*(D\pi)\ell\bar{\nu}_\ell$

Pietro Colangelo,^{1,*} Fulvia De Fazio,^{1,†} Francesco Loporco,^{1,‡} and Nicola Losacco^{1,2,§}

¹*Istituto Nazionale di Fisica Nucleare, Sezione di Bari, via Orabona 4, 70126 Bari, Italy*

²*Dipartimento Interateneo di Fisica "Michelangelo Merlin",
Università degli Studi di Bari, via Orabona 4, 70126 Bari, Italy*

The Belle Collaboration has recently measured the complete set of angular coefficient functions for the exclusive decays $\bar{B} \rightarrow D^*(D\pi)\ell\bar{\nu}_\ell$, with $\ell = e, \mu$, in four bins of the parameter $w = \frac{m_B^2 + m_{D^*}^2 - q^2}{2m_B m_{D^*}}$, with q the lepton pair momentum [1]. Under the assumption that physics beyond the Standard Model does not contribute to such modes, the measurements are useful to determine the hadronic form factors describing the $B \rightarrow D^*$ matrix elements of the Standard Model weak current, and to improve the determination of $|V_{cb}|$. On the other hand, they can be used to assess the impact of possible new physics contributions. In a bottom-up approach, we extend the Standard Model effective Hamiltonian governing this mode with the inclusion of the full set of Lorentz invariant d=6 operators compatible with the gauge symmetry of the theory. The measured angular coefficient functions can tightly constrain the couplings in the generalized Hamiltonian. We present the first results of this analysis, discussing how improvements can be achieved when more complete data on the angular coefficient functions will be available.

I. INTRODUCTION AND FRAMEWORK

In the search of signals from physics beyond the Standard Model (SM), a few tensions between SM expectations and measurements have emerged in the flavour sector [2, 3]. In particular, in addition to processes suppressed at tree-level in SM, which are highly sensitive to virtual contribution of heavy quanta [4], also charged current processes are under scrutiny after the emergence of anomalies in the ratios $R(D^{(*)}) = \frac{\mathcal{B}(B \rightarrow D^{(*)}\tau\nu_\tau)}{\mathcal{B}(B \rightarrow D^{(*)}\ell\nu_\ell)}$ ($\ell = e, \mu$) in BaBar Collaboration [5] and subsequent analyses [6–12] (see [2, 13] for averages and review). The possibility of relating such anomalies to the tensions for the different determinations of $|V_{cb}|$ makes the investigation of such processes even more intriguing [14].

The angular coefficient functions in the fully differential $\bar{B}(p) \rightarrow D^{(*)}(p', \epsilon)(D\pi)\ell(k_1)\bar{\nu}_\ell(k_2)$ decay distribution are suitable observables to look for the effects of new physics (NP) [15–19]. The Belle Collaboration has recently reported the measurement of the complete set of such functions in four bins of the hadronic recoil parameter $w = \frac{m_B^2 + m_{D^*}^2 - q^2}{2m_B m_{D^*}}$, with $q = p - p'$ [1]. Here, we want to consider the role of NP in this process using theoretical expressions that can be applied also to other modes [20, 21]. We make use of the Standard Model effective field theory (SMEFT) as a model-independent framework to

analyze NP contributions to beauty hadron decays [22, 23]. If the NP scale Λ_{NP} is much larger than the electroweak scale, the new massive degrees of freedom can be integrated out providing an effective Hamiltonian in terms of SM fields, invariant under the SM gauge group. In the extended Hamiltonian new operators not present in the SM appear, suppressed by powers of $1/\Lambda_{NP}$. At $\mathcal{O}(1/\Lambda_{NP}^2)$ these are dimension-six operators. Among these, those relevant for the present study are four fermion operators.

To describe the modes $\bar{B} \rightarrow V\ell^-\bar{\nu}_\ell$, with V a meson comprising an up-type quark U , we consider the generalized effective Hamiltonian

$$\begin{aligned}
 H_{\text{eff}}^{b \rightarrow U\ell\nu} &= \frac{G_F}{\sqrt{2}} V_{Ub} \\
 &\times \left\{ (1 + \epsilon_V^\ell) (\bar{U}\gamma_\mu(1 - \gamma_5)b) (\bar{\ell}\gamma^\mu(1 - \gamma_5)\nu_\ell) \right. \\
 &+ \epsilon_R^\ell (\bar{U}\gamma_\mu(1 + \gamma_5)b) (\bar{\ell}\gamma^\mu(1 - \gamma_5)\nu_\ell) \\
 &+ \epsilon_S^\ell (\bar{U}b) (\bar{\ell}(1 - \gamma_5)\nu_\ell) + \epsilon_P^\ell (\bar{U}\gamma_5b) (\bar{\ell}(1 - \gamma_5)\nu_\ell) \\
 &\left. + \epsilon_T^\ell (\bar{U}\sigma_{\mu\nu}(1 - \gamma_5)b) (\bar{\ell}\sigma^{\mu\nu}(1 - \gamma_5)\nu_\ell) \right\} + h.c. ,
 \end{aligned} \tag{1}$$

with G_F the Fermi constant and V_{Ub} the relevant element of the Cabibbo-Kobayashi-Maskawa (CKM) matrix. Besides the SM term, the low energy Hamiltonian (1) comprises NP operators with complex $\epsilon_{V,R,S,P,T}^\ell$ lepton-flavour dependent coefficients. The scalar operator does not contribute if V is a vector meson, as D^* in the present case.

We choose the kinematics indicated in Fig. 1: θ_V is the angle between the D meson and the direction opposite to the \bar{B} in the D^* rest frame; θ_ℓ the angle between the charged lepton and the \bar{B} in the vir-

* Electronic address:pietro.colangelo@ba.infn.it

† Electronic address:fulvia.defazio@ba.infn.it

‡ Electronic address:francesco.loporco1@ba.infn.it

§ Electronic address:nicola.losacco@ba.infn.it

tual W rest frame and ϕ the angle between the decay planes identified by the directions of the lepton pair on one hand and the (D, π) pair on the other in the \bar{B} rest frame. Using such variables the fully differential decay width reads:

$$\begin{aligned} \frac{d^4\Gamma(\bar{B} \rightarrow V(P_1P_2)\ell^-\bar{\nu}_\ell)}{dq^2 d\cos\theta d\phi d\cos\theta_V} &= \mathcal{C}|\vec{p}_V| \left(1 - \frac{m_\ell^2}{q^2}\right)^2 \\ &\times \left\{ I_{1s} \sin^2\theta_V + I_{1c} \cos^2\theta_V \right. \\ &+ (I_{2s} \sin^2\theta_V + I_{2c} \cos^2\theta_V) \cos 2\theta \\ &+ I_3 \sin^2\theta_V \sin^2\theta \cos 2\phi + I_4 \sin 2\theta_V \sin 2\theta \cos \phi \\ &+ I_5 \sin 2\theta_V \sin \theta \cos \phi \\ &+ (I_{6s} \sin^2\theta_V + I_{6c} \cos^2\theta_V) \cos \theta \\ &+ I_7 \sin 2\theta_V \sin \theta \sin \phi + I_8 \sin 2\theta_V \sin 2\theta \sin \phi \\ &\left. + I_9 \sin^2\theta_V \sin^2\theta \sin 2\phi \right\}, \end{aligned} \quad (2)$$

with $\mathcal{C} = \frac{3G_F^2|V_{Ub}|^2\mathcal{B}(V \rightarrow P_1P_2)}{128(2\pi)^4m_B^2}$ and \vec{p}_V the three-momentum of the V meson (here D^*) in the B meson rest-frame. The angular coefficient functions I_i in (2) depend on the couplings $\epsilon_{V,R,P,T}^\ell$, on q^2 (or w) and on the hadronic form factors:

$$\begin{aligned} I_i &= |1 + \epsilon_V|^2 I_i^{SM} + |\epsilon_R|^2 I_i^{NP,R} + |\epsilon_P|^2 I_i^{NP,P} \\ &+ |\epsilon_T|^2 I_i^{NP,T} + 2\text{Re}[\epsilon_R(1 + \epsilon_V^*)] I_i^{INT,R} \\ &+ 2\text{Re}[\epsilon_P(1 + \epsilon_V^*)] I_i^{INT,P} \\ &+ 2\text{Re}[\epsilon_T(1 + \epsilon_V^*)] I_i^{INT,T} \\ &+ 2\text{Re}[\epsilon_R\epsilon_T^*] I_i^{INT,RT} + 2\text{Re}[\epsilon_P\epsilon_T^*] I_i^{INT,PT} \\ &+ 2\text{Re}[\epsilon_P\epsilon_R^*] I_i^{INT,PR} \end{aligned} \quad (3)$$

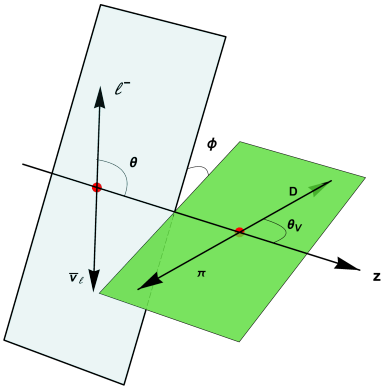


FIG. 1. Kinematics of $\bar{B} \rightarrow D^*(D\pi)\ell^-\bar{\nu}_\ell$.

for $i = 1s, \dots, 6c$,

$$\begin{aligned} I_7 &= 2\text{Im}[\epsilon_R(1 + \epsilon_V^*)] I_7^{INT,R} \\ &+ 2\text{Im}[\epsilon_P(1 + \epsilon_V^*)] I_7^{INT,P} \\ &+ 2\text{Im}[\epsilon_T(1 + \epsilon_V^*)] I_7^{INT,T} \\ &+ 2\text{Im}[\epsilon_R\epsilon_T^*] I_7^{INT,RT} + 2\text{Im}[\epsilon_P\epsilon_T^*] I_7^{INT,PT} \\ &+ 2\text{Im}[\epsilon_P\epsilon_R^*] I_7^{INT,PR}, \end{aligned} \quad (4)$$

and for $i = 8, 9$

$$I_i = 2\text{Im}[\epsilon_R(1 + \epsilon_V^*)] I_i^{INT,R}. \quad (5)$$

In SM such functions are expressed in terms of helicity amplitudes:

$$\begin{aligned} H_0 &= \frac{1}{2m_V(m_B + m_V)\sqrt{q^2}} \\ &\left((m_B + m_V)^2(m_B^2 - m_V^2 - q^2)A_1(q^2) \right. \\ &\left. - \lambda(m_B^2, m_V^2, q^2)A_2(q^2) \right) \end{aligned} \quad (6)$$

$$\begin{aligned} H_{\pm} &= \frac{(m_B + m_V)^2 A_1(q^2) \mp \sqrt{\lambda(m_B^2, m_V^2, q^2)} V(q^2)}{m_B + m_V} \\ H_t &= -\frac{\sqrt{\lambda(m_B^2, m_V^2, q^2)}}{\sqrt{q^2}} A_0(q^2), \end{aligned}$$

with the form factors defined in the appendix A. For NP operators the amplitudes are also introduced:

$$\begin{aligned} H_{\pm}^{NP} &= \frac{1}{\sqrt{q^2}} \left\{ q^2(T_1(q^2) - T_2(q^2)) \right. \\ &\left. + (m_B^2 - m_V^2 \pm \sqrt{\lambda(m_B^2, m_V^2, q^2)}) (T_1(q^2) + T_2(q^2)) \right\} \\ H_L^{NP} &= 4 \left\{ \frac{\lambda(m_B^2, m_V^2, q^2)}{m_V(m_B + m_V)^2} T_0(q^2) \right. \\ &\left. + 2 \frac{m_B^2 + m_V^2 - q^2}{m_V} T_1(q^2) + 4m_V T_2(q^2) \right\}. \end{aligned} \quad (7)$$

The form factors T_i are also defined in appendix A. The expressions of all coefficient functions I_i are in Tables I-V included the appendix B.

II. CONSTRAINTS ON NP COUPLINGS FROM BELLE MEASUREMENT

The comparison of the Belle measurement [1] to the theoretical expressions in the previous section allows us to constrain the couplings in the generalized Hamiltonian (1). Before presenting the analysis, we point out that i) the coefficient functions

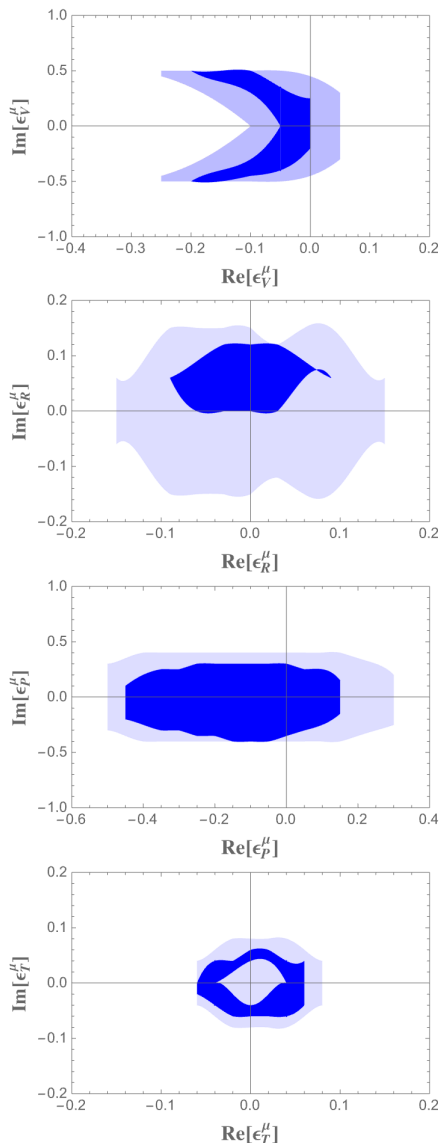


FIG. 2. NP couplings ϵ_V^μ , ϵ_R^μ , ϵ_P^μ , ϵ_T^μ obtained from the Belle measurement of the angular coefficient functions of $\bar{B} \rightarrow D^*(D\pi)\mu^-\bar{\nu}_\mu$. The light region corresponds to requiring that the theoretical results agree with the experimental data at 2.5σ . The dark region corresponds to the values obtained minimizing the reduced χ^2 .

defined in the previous section are related to the coefficient functions in [1], denoted as J_i , through $|I_i| = |J_i/F|$, with $F = \frac{3|\vec{p}_{D^*}|}{2^{10}m_B^5}$; ii) the angle θ_ℓ in [1] corresponds to $\theta_\ell \rightarrow \pi - \theta$ in our notation, therefore we have $I_i = -J_i/F$ for $i = 4, 6s, 6c, 8$, and $I_i = J_i/F$ for all the other coefficients; iii) the Belle Collaboration provides the angular coefficient functions in four bins $\Delta w^{(a)}$ of w , defining $\bar{J}_i^a = \int_{\Delta w^{(a)}} J_i(w)dw$ and $\hat{J}_i = J_i/\mathcal{N}$, where $\mathcal{N} =$

$\frac{8}{9}\pi \sum_{a=1}^4 (3\bar{J}_{1c}^a + 6\bar{J}_{1s}^a - \bar{J}_{2c}^a - 2\bar{J}_{2s}^a)$. The factor \mathcal{N} corresponds, modulo a constant, to the integrated width.

To get information on the effective couplings we proceed as follows. From Fig. 1 of [1] we obtain the values of the coefficients \hat{J}_i in the four bins $\Delta w^{(1)} = [1, 1.15]$, $\Delta w^{(2)} = [1.15, 1.25]$, $\Delta w^{(3)} = [1.25, 1.35]$, $\Delta w^{(4)} = [1.35, 1.5]$ (for such an information the Collaboration has not provided in [1] the table of numerical results and the error covariance matrix). Next, we consider the products $(\hat{J}_i^a)_{\text{int}}^{\text{exp}} = \hat{J}_i \cdot (\Delta w)^a$. Using the results in appendix B and fixing the parameter $\mathcal{N} = 0.146$ to reproduce the measured branching ratio quoted in [24], we calculate the expressions of the integrals of the coefficient functions in each bin of w , $(\hat{J}_i^a)_{\text{int}}^{\text{th}}$. The w dependence of the hadronic form factors is needed to perform the integrals: we use the CLN parametrization [25] with the parameters obtained in [26]. The details on the reconstruction of the form factors and on the choice of the parameters can be found in [15].

We require that $(\hat{J}_i^a)_{\text{int}}^{\text{th}} \in [(\hat{J}_i^a)_{\text{int}}^{\text{exp}} - k\sigma_i^a, (\hat{J}_i^a)_{\text{int}}^{\text{exp}} + k\sigma_i^a]$, with k a number of standard deviations to be fixed; σ_i^a is the error of the Belle result for each \hat{J}_i^a multiplied by the corresponding bin width. We have a total of 48 constraints, i.e. the integrals over 4 bins for 12 angular coefficients. Since the data refer to the muon channel, we determine the set $(\epsilon_V^\mu, \epsilon_R^\mu, \epsilon_P^\mu, \epsilon_T^\mu)$ (set 1) that can simultaneously satisfy all constraints, within the initial ranges $|\epsilon_i^\mu| \leq 0.5$ for $i = V, R, P, T$. We find that the smallest value of k for which all constraints are fulfilled is $k = 2.5$. For this set of parameters we compute the function $\chi_{red}^2 = \frac{1}{N_{dof}} \sum_{i,a} \left((\hat{J}_i^a)_{\text{int}}^{\text{th}} - (\hat{J}_i^a)_{\text{int}}^{\text{exp}} \right)^2 / (\sigma_i^a)^2$, with $N_{dof} = 40$, $i = 1s, \dots, 9$ and $a = 1, \dots, 4$. The values of this function lie in the range $[1.8, 2.6]$, the minimum corresponds to the set of parameters $(\text{Re}[\epsilon_V], \text{Im}[\epsilon_V]) = (-0.05, 0.25)$; $(\text{Re}[\epsilon_R], \text{Im}[\epsilon_R]) = (-0.03, 0.09)$; $(\text{Re}[\epsilon_P], \text{Im}[\epsilon_P]) = (-0.25, -0.25)$; $(\text{Re}[\epsilon_T], \text{Im}[\epsilon_T]) = (0.04, -0.04)$. To be conservative we select more points, those satisfying $\chi_{red}^2 \leq 1.875$ (set 2). This choice is sensible since the probability to find $\chi_{red}^2 > 1.875$ in the case of 40 degrees of freedom is 0.07%. For comparison, the SM case (i.e. $\epsilon_V = \epsilon_R = \epsilon_P = \epsilon_T = 0$ and $N_{dof} = 48$) corresponds to $\chi_{red}^2 = 2$. The results are in Fig. 2: the light region corresponds to the parameters in set 1, while the dark region to the parameters in set 2. The agreement with data can be appreciated from Fig. 3 which includes the Belle points together with the angular coefficient functions obtained using the determined ϵ couplings. The remarkable result is that, while the SM point with all new couplings equal to zero is allowed, it does not belong to the region of minimum χ^2 , and

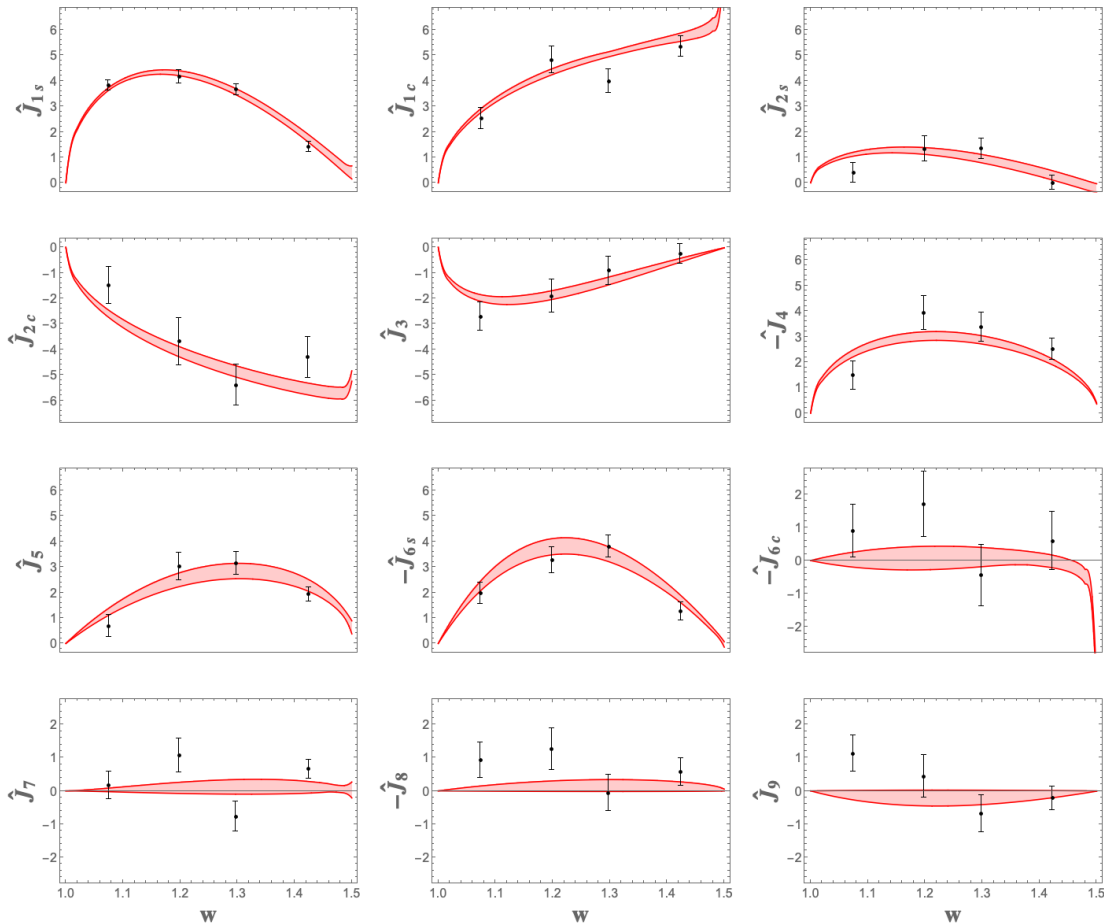


FIG. 3. Angular coefficient functions in Eq. (2) for $\bar{B} \rightarrow D^*(D\pi)\mu^- \bar{\nu}_\mu$. The shaded regions correspond to the results obtained using the determined ϵ couplings, the points are the Belle measurements [1].

there is the possibility of values different from zero in ϵ_T^μ . This observation will be strengthened when

Other observables are sensitive to the effects of the new operators in (1). In particular, an interesting observable is the ratio

$$R_{21s}(w) = \frac{\hat{J}_{2s}(w)}{\hat{J}_{1s}(w)}. \quad (8)$$

Indeed, as obtained using the expressions in appendix B, the angular coefficient functions $I_{1s, 2s}$, hence $\hat{J}_{1s, 2s}$, do not depend on ϵ_P . For vanishing ϵ_T their ratio would be independent of the form factors and insensitive to ϵ_V, ϵ_R . Therefore, the ratio (8) might signal the tensor operator. This is displayed in Fig. 4 which shows that for nonvanishing ϵ_T the ratio can have a zero for w_0 in the range [1.44, 1.5] in the muon channel.

The structure of the angular coefficients provides insights on the possibility that ϵ_T is the only nonva-

the table of measurements and the error covariance matrix will be available.

nishing new coupling. In particular, for $\epsilon_V = \epsilon_R = 0$

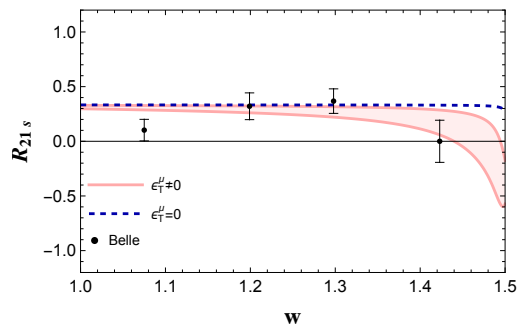


FIG. 4. Ratio R_{21s} in Eq. (8) for $\epsilon_T^\mu = 0$ (dashed line) and varying ϵ_T^μ in the range displayed in Fig. 2 (shaded region).

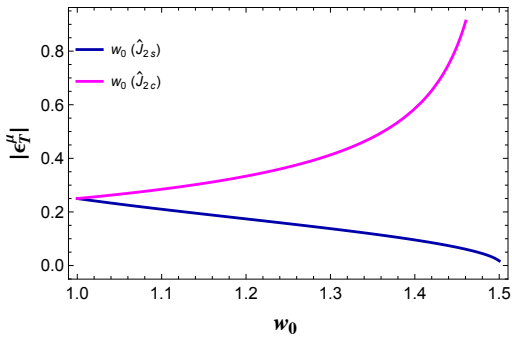


FIG. 5. $|\epsilon_T^\mu|$ as a function of the position of the zero of the ratio \hat{J}_{2s} (blue curve) and \hat{J}_{2c} (magenta curve) for $\epsilon_V^\mu = \epsilon_R^\mu = 0$.

one finds that both \hat{J}_{2s} and \hat{J}_{2c} might have a zero. This is depicted in Fig. 5. This figure shows that if $|\epsilon_T^\mu| < 0.25$ \hat{J}_{2s} should have a zero while \hat{J}_{2c} should not, and viceversa. They cannot have a zero simultaneously. Although the Belle data are not precise enough to draw definite conclusions, they seem to exclude the presence of a zero in \hat{J}_{2c} and are compatible with the presence of a zero of \hat{J}_{2s} in the last bin of w . Other angular coefficient functions provide us with further information. If the only nonvanishing NP coupling is ϵ_T , \hat{J}_{6c} would display a zero at a value given by the relation

$$\sqrt{q^2} H_L^{\text{NP}}(q^2) \text{Re}[\epsilon_T] - 4m_\ell H_0(q^2) = 0. \quad (9)$$

The position w_0 of the zero of \hat{J}_{6c} would fix $\text{Re}[\epsilon_T]$. This is shown in Fig. 6, where the continuous curve corresponds to the relation (9), while the gray band is the range of w where the zero of \hat{J}_{6c} should be

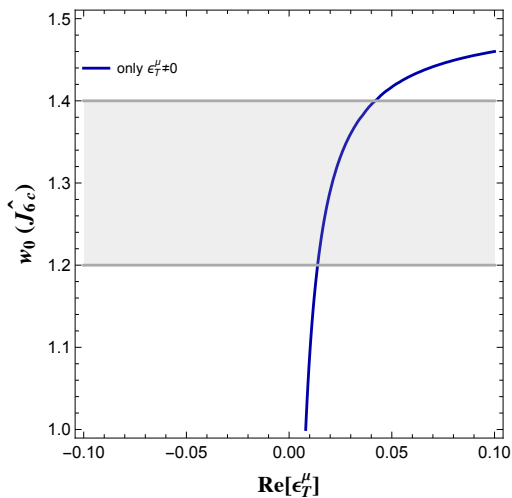


FIG. 6. $\text{Re}[\epsilon_T^\mu]$ as a function of the position of the zero of \hat{J}_{6c} for $\epsilon_V^\mu = \epsilon_R^\mu = \epsilon_P^\mu = 0$, obtained from Eq. (9).

found according to the Belle measurement. This corresponds to small values of $\text{Re}[\epsilon_T^\mu]$, consistently with the results for \hat{J}_{2s} and \hat{J}_{2c} .

III. CONCLUSIONS

The measurement of the full set of angular coefficient functions in $\bar{B} \rightarrow D^*(D\pi)\mu\bar{\nu}_\mu$ constrains the set of NP coefficients in the generalized low energy Hamiltonian. In particular, the possibility that some NP coefficients are different from zero emerges as a first evidence on the basis of the information available in [1]. It will be possible to corroborate this indication using the experimental table of measurements together with the covariance error matrix.

Note added. When this manuscript was completed, the paper [27] was uploaded to the archive, dealing with the same issue.

Acknowledgements. We thank M. Prim and M. Rotondo for discussions. This study has been carried out within the INFN project (Iniziativa Specifica) SPIF. The research has been partly funded by the European Union – Next Generation EU through the research Grant No. P2022Z4P4B “SOPHYA - Sustainable Optimised PHYSICS Algorithms: fundamental physics to build an advanced society” under the program PRIN 2022 PNRR of the Italian Ministero dell’Università e Ricerca (MUR).

Appendix A: Hadronic matrix elements

The $\bar{B} \rightarrow V$ matrix elements are parametrized as:

$$\begin{aligned} \langle V(p', \epsilon) | \bar{U} \gamma_\mu b | B(p) \rangle &= -\frac{2V(q^2)}{m_B + m_V} i\epsilon_{\mu\nu\alpha\beta} \epsilon^{*\nu} p^\alpha p'^\beta, \\ \langle V(p', \epsilon) | \bar{U} \gamma_\mu \gamma_5 b | B(p) \rangle &= \\ (m_B + m_V) \left(\epsilon_\mu^* - \frac{(\epsilon^* \cdot q)}{q^2} q_\mu \right) A_1(q^2) \\ - \frac{(\epsilon^* \cdot q)}{m_B + m_V} \left((p + p')_\mu - \frac{m_B^2 - m_V^2}{q^2} q_\mu \right) A_2(q^2) \\ + (\epsilon^* \cdot q) \frac{2m_V}{q^2} q_\mu A_0(q^2), \quad (\text{A.1}) \\ \langle V(p', \epsilon) | \bar{U} \gamma_5 b | B(p) \rangle &= -\frac{2m_V}{m_b + m_U} (\epsilon^* \cdot q) A_0(q^2), \end{aligned}$$

with the condition

$$A_0(0) = \frac{m_B + m_V}{2m_V} A_1(0) - \frac{m_B - m_V}{2m_V} A_2(0), \quad (\text{A.2})$$

and

$$\begin{aligned}
& \langle V(p', \epsilon) | \bar{U} \sigma_{\mu\nu} b | B(p) \rangle = \\
& T_0(q^2) \frac{\epsilon^* \cdot q}{(m_B + m_V)^2} \epsilon_{\mu\nu\alpha\beta} p^\alpha p'^\beta \\
& + T_1(q^2) \epsilon_{\mu\nu\alpha\beta} p^\alpha \epsilon^{*\beta} + T_2(q^2) \epsilon_{\mu\nu\alpha\beta} p'^\alpha \epsilon^{*\beta}, \\
& \langle V(p', \epsilon) | \bar{U} \sigma_{\mu\nu} \gamma_5 b | B(p) \rangle = \tag{A.3} \\
& i T_0(q^2) \frac{\epsilon^* \cdot q}{(m_B + m_V)^2} (p_\mu p'_\nu - p_\nu p'_\mu) \\
& + i T_1(q^2) (p_\mu \epsilon_\nu^* - \epsilon_\mu^* p_\nu) + i T_2(q^2) (p'_\mu \epsilon_\nu^* - \epsilon_\mu^* p'_\nu).
\end{aligned}$$

Appendix B: Angular coefficient functions

TABLE I. Angular coefficient functions in the 4d $\bar{B} \rightarrow V(P_1 P_2) \ell^- \bar{\nu}_\ell$ decay distribution for the SM.

i	I_i^{SM}
I_{1s}	$\frac{1}{2}(H_+^2 + H_-^2)(m_\ell^2 + 3q^2)$
I_{1c}	$4m_\ell^2 H_t^2 + 2H_0^2(m_\ell^2 + q^2)$
I_{2s}	$-\frac{1}{2}(H_+^2 + H_-^2)(m_\ell^2 - q^2)$
I_{2c}	$2H_0^2(m_\ell^2 - q^2)$
I_3	$2H_+ H_- (m_\ell^2 - q^2)$
I_4	$H_0(H_+ + H_-)(m_\ell^2 - q^2)$
I_5	$-2H_t(H_+ + H_-)m_\ell^2 - 2H_0(H_+ - H_-)q^2$
I_{6s}	$2(H_+^2 - H_-^2)q^2$
I_{6c}	$-8H_t H_0 m_\ell^2$
I_7	0
I_8	0
I_9	0

[1] M. T. Prim *et al.* (Belle), (2023), arXiv:2310.20286 [hep-ex].
[2] Y. Amhis *et al.*, Phys. Rev. D **107**, 052008 (2023), arXiv:2206.07501 [hep-ex].

[3] F. De Fazio (2023) arXiv:2311.02987 [hep-ph].
[4] A. Buras, *Gauge Theory of Weak Decays* (Cambridge University Press, 2020).
[5] J. P. Lees *et al.* (BaBar), Phys. Rev. Lett. **109**,

TABLE II. Angular coefficient functions for $\bar{B} \rightarrow V(P_1 P_2)\ell^- \bar{\nu}_\ell$: NP term with the R operator, and interference SM-NP with R operator.

i	$I_i^{\text{NP},R}$	$I_i^{\text{INT},R}$
I_{1s}	$\frac{1}{2}(H_+^2 + H_-^2)(m_\ell^2 + 3q^2)$	$-H_- H_+(m_\ell^2 + 3q^2)$
I_{1c}	$4m_\ell^2 H_t^2 + 2H_0^2(m_\ell^2 + q^2)$	$-2(2H_t^2 m_\ell^2 + H_0^2(m_\ell^2 + q^2))$
I_{2s}	$-\frac{1}{2}(H_+^2 + H_-^2)(m_\ell^2 - q^2)$	$H_- H_+(m_\ell^2 - q^2)$
I_{2c}	$2H_0^2(m_\ell^2 - q^2)$	$-2H_0^2(m_\ell^2 - q^2)$
I_3	$2H_+ H_-(m_\ell^2 - q^2)$	$-(H_+^2 + H_-^2)(m_\ell^2 - q^2)$
I_4	$H_0(H_+ + H_-)(m_\ell^2 - q^2)$	$-H_0(H_+ + H_-)(m_\ell^2 - q^2)$
I_5	$-2H_t(H_+ + H_-)m_\ell^2 + 2H_0(H_+ - H_-)q^2$	$2H_t(H_+ + H_-)m_\ell^2$
I_{6s}	$-2(H_+^2 - H_-^2)q^2$	0
I_{6c}	$-8H_t H_0 m_\ell^2$	$8H_0 H_t m_\ell^2$
I_7	0	$2(H_+ - H_-)H_t m_\ell^2$
I_8	0	$-H_0(H_+ - H_-)(m_\ell^2 - q^2)$
I_9	0	$-(H_+^2 - H_-^2)(m_\ell^2 - q^2)$

TABLE III. Angular coefficient functions for $\bar{B} \rightarrow V(P_1 P_2)\ell^- \bar{\nu}_\ell$: NP term with the P operator, and interference SM-NP with P operator.

i	$I_i^{\text{NP},P}$	$I_i^{\text{INT},P}$
I_{1s}	0	0
I_{1c}	$4H_t^2 \frac{q^4}{(m_b + m_U)^2}$	$4H_t^2 \frac{m_\ell q^2}{m_b + m_U}$
I_{2s}	0	0
I_{2c}	0	0
I_3	0	0
I_4	0	0
I_5	0	$-H_t(H_+ + H_-) \frac{m_\ell q^2}{m_b + m_U}$
I_{6s}	0	0
I_{6c}	0	$-4H_t H_0 \frac{m_\ell q^2}{m_b + m_U}$
I_7	0	$-H_t(H_+ - H_-) \frac{m_\ell q^2}{m_b + m_U}$
I_8	0	0
I_9	0	0

TABLE IV. Angular coefficient functions for $\bar{B} \rightarrow V(P_1 P_2) \ell^- \bar{\nu}_\ell$: NP term with the T operator and interference SM-NP with T operator.

i	$I_i^{\text{NP},T}$	$I_i^{\text{INT},T}$
I_{1s}	$2[(H_+^{\text{NP}})^2 + (H_-^{\text{NP}})^2](3m_\ell^2 + q^2)$	$-4(H_+^{\text{NP}} H_+ + H_-^{\text{NP}} H_-)m_\ell \sqrt{q^2}$
I_{1c}	$\frac{1}{8}(H_L^{\text{NP}})^2(m_\ell^2 + q^2)$	$-H_L^{\text{NP}} H_0 m_\ell \sqrt{q^2}$
I_{2s}	$2[(H_+^{\text{NP}})^2 + (H_-^{\text{NP}})^2](m_\ell^2 - q^2)$	0
I_{2c}	$\frac{1}{8}(H_L^{\text{NP}})^2(q^2 - m_\ell^2)$	0
I_3	$8H_+^{\text{NP}} H_-^{\text{NP}}(q^2 - m_\ell^2)$	0
I_4	$\frac{1}{2}H_L^{\text{NP}}(H_+^{\text{NP}} + H_-^{\text{NP}})(q^2 - m_\ell^2)$	0
I_5	$-H_L^{\text{NP}}(H_+^{\text{NP}} - H_-^{\text{NP}})m_\ell^2$	$\frac{1}{4}[H_L^{\text{NP}}(H_+ - H_-) + 8H_+^{\text{NP}}(H_t + H_0) + 8H_-^{\text{NP}}(H_t - H_0)]m_\ell \sqrt{q^2}$
I_{6s}	$8[(H_+^{\text{NP}})^2 - (H_-^{\text{NP}})^2]m_\ell^2$	$-4(H_+^{\text{NP}} H_+ - H_-^{\text{NP}} H_-)m_\ell \sqrt{q^2}$
I_{6c}	0	$H_L^{\text{NP}} H_t m_\ell \sqrt{q^2}$
I_7	0	$\frac{1}{4}[H_L^{\text{NP}}(H_+ + H_-) - 8H_+^{\text{NP}}(H_t + H_0) + 8H_-^{\text{NP}}(H_t - H_0)]m_\ell \sqrt{q^2}$
I_8	0	0
I_9	0	0

TABLE V. Angular coefficient functions for $\bar{B} \rightarrow V(P_1 P_2) \ell^- \bar{\nu}_\ell$: P-R, R-T and P-T interferences.

i	$I_i^{\text{INT},PR}$	$I_i^{\text{INT},RT}$	$I_i^{\text{INT},PT}$
I_{1s}	0	$4(H_-^{\text{NP}} H_+ + H_- H_+^{\text{NP}})m_\ell \sqrt{q^2}$	0
I_{1c}	$-4H_t^2 m_\ell \frac{q^2}{m_b + m_U}$	$H_0 H_L^{\text{NP}} m_\ell \sqrt{q^2}$	0
I_{2s}	0	0	0
I_{2c}	0	0	0
I_3	0	0	0
I_4	0	0	0
I_5	$(H_+ + H_-)H_t m_\ell \frac{q^2}{m_b + m_U}$	$\frac{1}{4}[H_L^{\text{NP}}(H_+ - H_-) - 8H_+^{\text{NP}}(H_t + H_0) - 8H_-^{\text{NP}}(H_t - H_0)]m_\ell \sqrt{q^2}$	$2H_t(H_+^{\text{NP}} + H_-^{\text{NP}}) \frac{(q^2)^{3/2}}{m_b + m_U}$
I_{6s}	0	$4(-H_-^{\text{NP}} H_+ + H_- H_+^{\text{NP}})m_\ell \sqrt{q^2}$	0
I_{6c}	$4H_0 H_t m_\ell \frac{q^2}{m_b + m_U}$	$-H_t H_L^{\text{NP}} m_\ell \sqrt{q^2}$	$H_t H_L^{\text{NP}} \frac{(q^2)^{3/2}}{m_b + m_U}$
I_7	$-H_t(H_+ - H_-)m_\ell \frac{q^2}{m_b + m_U}$	$\frac{1}{4}[H_L^{\text{NP}}(H_+ + H_-) - 8H_+^{\text{NP}}(H_t + H_0) + 8H_-^{\text{NP}}(H_t - H_0)]m_\ell \sqrt{q^2}$	$2H_t(H_+^{\text{NP}} - H_-^{\text{NP}}) \frac{(q^2)^{3/2}}{m_b + m_U}$
I_8	0	0	0
I_9	0	0	0

- 101802 (2012), arXiv:1205.5442 [hep-ex].
- [6] J. P. Lees *et al.* (BaBar), Phys. Rev. D **88**, 072012 (2013), arXiv:1303.0571 [hep-ex].
- [7] M. Huschle *et al.* (Belle), Phys. Rev. D **92**, 072014 (2015), arXiv:1507.03233 [hep-ex].
- [8] R. Aaij *et al.* (LHCb), Phys. Rev. Lett. **115**, 111803 (2015), [Erratum: Phys.Rev.Lett. 115, 159901 (2015)], arXiv:1506.08614 [hep-ex].
- [9] S. Hirose *et al.* (Belle), Phys. Rev. Lett. **118**, 211801 (2017), arXiv:1612.00529 [hep-ex].
- [10] R. Aaij *et al.* (LHCb), Phys. Rev. Lett. **120**, 171802 (2018), arXiv:1708.08856 [hep-ex].
- [11] R. Aaij *et al.* (LHCb), Phys. Rev. D **97**, 072013 (2018), arXiv:1711.02505 [hep-ex].
- [12] G. Caria *et al.* (Belle), Phys. Rev. Lett. **124**, 161803 (2020), arXiv:1910.05864 [hep-ex].
- [13] P. Gambino *et al.*, Eur. Phys. J. C **80**, 966 (2020), arXiv:2006.07287 [hep-ph].
- [14] P. Colangelo and F. De Fazio, Phys. Rev. **D95**, 011701 (2017), arXiv:1611.07387 [hep-ph].
- [15] P. Colangelo and F. De Fazio, JHEP **06**, 082 (2018), arXiv:1801.10468 [hep-ph].
- [16] S. Bhattacharya, S. Nandi, and S. Kumar Patra, Eur. Phys. J. C **79**, 268 (2019), arXiv:1805.08222 [hep-ph].
- [17] C. Murgui, A. Peñuelas, M. Jung, and A. Pich, JHEP **09**, 103 (2019), arXiv:1904.09311 [hep-ph].
- [18] D. Bečirević, M. Fedele, I. Nišandžić, and A. Tayduganov, (2019), arXiv:1907.02257 [hep-ph].
- [19] C. Bobeth, M. Bordone, N. Gubernari, M. Jung, and D. van Dyk, Eur. Phys. J. C **81**, 984 (2021), arXiv:2104.02094 [hep-ph].
- [20] P. Colangelo, F. De Fazio, and F. Lopalco, Phys. Rev. D **100**, 075037 (2019), arXiv:1906.07068 [hep-ph].
- [21] P. Colangelo, F. De Fazio, and F. Lopalco, Phys. Rev. D **103**, 075019 (2021), arXiv:2102.05365 [hep-ph].
- [22] W. Buchmuller and D. Wyler, Nucl. Phys. **B268**, 621 (1986).
- [23] B. Grzadkowski, M. Iskrzynski, M. Misiak, and J. Rosiek, JHEP **10**, 085 (2010), arXiv:1008.4884 [hep-ph].
- [24] R. L. Workman and Others (Particle Data Group), PTEP **2022**, 083C01 (2022).
- [25] I. Caprini, L. Lellouch, and M. Neubert, Nucl. Phys. B **530**, 153 (1998), arXiv:hep-ph/9712417.
- [26] A. Abdesselam *et al.* (Belle), (2017), arXiv:1702.01521 [hep-ex].
- [27] T. Kapoor, Z.-R. Huang, and E. Kou, (2024), arXiv:2401.11636 [hep-ph].